

Provided for non-commercial research and education use.
Not for reproduction, distribution or commercial use.



This article appeared in a journal published by Elsevier. The attached copy is furnished to the author for internal non-commercial research and education use, including for instruction at the authors institution and sharing with colleagues.

Other uses, including reproduction and distribution, or selling or licensing copies, or posting to personal, institutional or third party websites are prohibited.

In most cases authors are permitted to post their version of the article (e.g. in Word or Tex form) to their personal website or institutional repository. Authors requiring further information regarding Elsevier's archiving and manuscript policies are encouraged to visit:

<http://www.elsevier.com/copyright>

Contents lists available at [SciVerse ScienceDirect](http://www.sciencedirect.com)

Quaternary Science Reviews

journal homepage: www.elsevier.com/locate/quascirev

Dynamic boundary-monsoon intensity hypothesis: evidence from the deglacial Amazon River discharge record

M.A. Maslin^{a,*}, V.J. Ettwein^a, K.E. Wilson^a, T.P. Guilderson^{b,c}, S.J. Burns^d, M.J. Leng^{e,f}^a Environmental Change Research Centre, University College London, Pearson Building, Gower Street, London, WC1E 6BT, UK^b Center for Accelerator Mass Spectrometry, Lawrence Livermore National Laboratory, 7000 East Avenue, L-397 Livermore, CA 94550, USA^c Department of Ocean Sciences, University of California – Santa Cruz, 1156 High Street, Santa Cruz, CA 95064, USA^d Department of Geosciences, 233 Morrill Science Center, University of Massachusetts Amherst, Amherst, MA 01003, USA^e Department of Geology, University of Leicester, Leicester, LE1 7RH, UK^f NERC Isotope Geosciences Laboratory, British Geological Survey, Nottingham, NG12 5GG, UK

ARTICLE INFO

Article history:

Received 7 February 2011

Received in revised form

18 October 2011

Accepted 19 October 2011

Available online 10 November 2011

Keywords:

Amazon Basin

Deglaciation

South American monsoon

Palaeoclimate

Amazon Fan sediment

Bi-polar climate forcing

ABSTRACT

Glacioeustatic- and temperature-corrected planktonic foraminiferal oxygen isotope ($\Delta\delta^{18}\text{O}$) records from ODP Site 942 on the Amazon Fan provide a means of monitoring past changes in the outflow of the Amazon River. This study focuses on the last deglaciation and reveals that during this period there were significant variations in the outflow, which implies large changes in moisture availability in the Amazon Basin. Aridity in the Amazon Basin seems to occur between 20.5 ka (calendar) to 17.0 ka and 13.6 ka to 11 ka. The second arid period correlates with the start of the Antarctic Cold Reversal and aridity continues throughout the Younger Dryas period. We find that the large-scale trends in Amazon River outflow are dissimilar to high-latitude variability in either hemisphere. Instead high-resolution variations correlate with the $\delta^{18}\text{O}$ difference between Greenland and Antarctica ice core temperature records. This suggests a link between Hemispheric temperature gradients and moisture availability over the Amazon. Based on our results and previously published work we present a new testable 'dynamic boundary-monsoon intensity hypothesis', which suggests that tropical moisture is not a simple belt that moves north or south. Rather, the northern and southern boundaries of the South American Summer Monsoon (SASM) are independently dynamic and driven by temperature gradients within their individual hemispheres. The intensity of rainfall within the SASM, however, is driven by precessionally modulated insolation and the resultant convection strength. Combining these two influences produces the dynamic heterogenic changes in the moisture availability observed over tropical South America since the Last Glacial Maximum.

© 2011 Elsevier Ltd. All rights reserved.

1. Introduction

The Amazon Basin represents the largest and most intense land-based convection centre on Earth and has a significant impact on extratropical atmospheric circulation (Barry and Chorley, 1995; Marengo and Nobre, 2001). It is drained by the Amazon River, which discharges approximately 20% of all freshwater transported to the oceans and has the largest drainage basin in the world covering an area of 7,050,000 km² (Franzini and Potter, 1983). Freshwater discharge from the Amazon River exceeds 6300 km³/yr

(~0.2 Sv) and carries with it nearly one Gt of sediment every year, over 80% of which originates in the Andes (Milliman and Meade, 1983). This massive output of sediment to the Atlantic Ocean is the primary reason for the extended continental shelf and the Amazon deep-sea fan complex. The Amazon Fan complex and associated sites were drilled by Ocean Drilling Program (ODP) Leg 155 (Flood et al., 1995). These sediments can provide a unique insight into long-term variations in the climate of the Amazon Basin, particularly in reconstructing the degree of cooling and aridity since the last glacial period (e.g., Damuth and Fairbanks, 1970; Flood et al., 1995; Haberle and Maslin, 1999; Maslin et al., 2005; Bendle et al., 2010). In this study we use planktonic foraminiferal $\delta^{18}\text{O}$ and Mg/Ca inferred sea surface temperature (SST) data from Ocean Drilling Program (ODP) Leg 155 Site 942 on the Amazon Fan to reconstruct past variations in Amazon River outflow, and infer long-term changes in the effective moisture balance

* Corresponding author. Department of Geography, University College London, Pearson Building, Gower Street, London, WC1E 6BT, UK. Tel.: +44 207 679 0556; fax: +44 207 679 0565.

E-mail address: m.maslin@ucl.ac.uk (M.A. Maslin).

(precipitation minus evaporation) of the Amazon Basin between 22 and 10 ka.

2. Background: Amazonian climatology

The Amazon Basin is a principal component of the global water cycle and forms an intrinsic part of many global climate mechanisms. Neotropical precipitation plays a fundamental role in the supply of latent heat to the high latitudes and determines the export of fresh water from the Atlantic Ocean to the Pacific Ocean, which is thought to regulate global thermohaline circulation (Marengo and Nobre, 2001; Vera et al., 2006; Leduc et al., 2007). Many researchers invoke changes in the seasonal positions of the Inter-tropical Convergence Zone (ITCZ) over both the oceans and continents to explain variations in neotropical rainfall patterns. This generalization is climatologically inaccurate when dealing with continental climate. Here, we refer to the South American Summer Monsoon (SASM) system (Fig. 1A), but note that it can be broadly related to the concept of the continental ITCZ (Lenters and Cook, 1997; Marengo and Nobre, 2001; Vera et al., 2006; Cook, 2009; see Fig. 1A and B) and also the South Atlantic convergence zone (SACZ) theory (Kodama, 1992; Carvalho et al., 2004; see Fig. 1A).

Between austral spring and summer, deep convective heating moves towards the South American Altiplano concurrent with the seasonal pattern of solar declination. (Zhou and Lau, 1998). The summer insolation maxima drives the formation of a persistent tropospheric closed anticyclone, the Bolivian High, which reverses surface wind circulation and leads to moisture import from the North Atlantic Ocean (Lenters and Cook, 1997). Intense diabatic heating, combined with enhanced latent heat release during frequent convective thunderstorms, induces a regional summer monsoon circulation regime, the SASM, which generates an intense and distinct rainy season over Amazonia between December and February (Lenters and Cook, 1997; Marengo and Nobre, 2001; Cook, 2009). In the SACZ model this is referred to as the Amazon sector (Fig. 1A) and nearly all of this rainfall is drained by the Amazon River system. The same intense continental heating also leads to stronger easterly winds that import of moisture air from the South Atlantic Ocean producing intense rainfall over South East Brazil, which is referred to as the Coastal sector (see Fig. 1A). The majority of this coastal rainfall is drained into the Atlantic Ocean by the Parana and the Sao Francisco rivers. There is very little connection between the Amazon and Coastal drainage basins. In contrast to South East Brazil, much of the Amazon Basin is relatively wet year-round with some regions, such as the northwest, experiencing

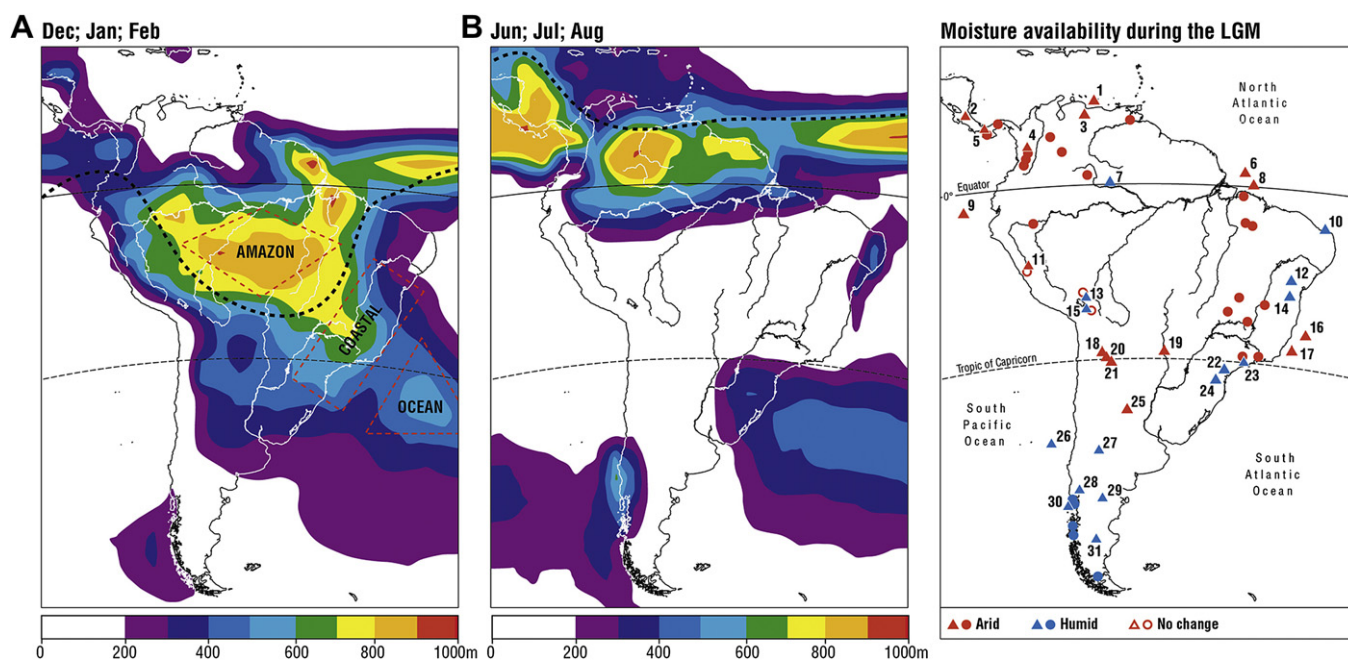


Fig. 1. Three maps showing the modern rainfall and location of key palaeo-data sites in South America. Long-term mean (1979–2000) Climate Prediction Center Merged Analysis of precipitation seasonal precipitation totals (in mm) for December–February (A) and June–August (B). 1A also shows the major features of the South Atlantic Convergence Zone (SACZ) the “Amazon”, “Coastal” and “Oceanic” sectors (Carvalho et al., 2004). The Amazon sector corresponds to the major rainfall over the Amazon Basin, which is also corresponds to the South America Summer Monsoon (SASM). Key South American rivers are illustrated to show the separate drainage basin in the Amazon and Coastal sectors. The mean hypothesised positions of the Inter-tropical convergence zone (dashed red line) are shown in A and B (Marengo and Nobre, 2001; Zhou and Lau, 1998; Carvalho et al., 2004). C. Locations of palaeoclimate records from the last glacial maximum and whether the authors found evidence for wetter (blue filled triangles/circles), drier (red filled triangles/circles) or no change (yellow open triangles/circles) compared to the present. Circles are used for key pollen records compiled by Marchant et al. (2009). 1. Cariaco Basin (Hughen et al., 1996; Peterson et al., 2000; Haug et al., 2001; Lea et al., 2003), 2. La Chonta Bog, Costa Rica (Islebe et al., 1995), 3. Lake Valencia, Venezuela (Leyden, 1985), 4. Lake Fuquene, Columbia (van der Hammen and Hooghiemstra, 2003), 5. El Valle Lake, Panama (Bush, 2002), 6. Amazon Fan (Damuth and Fairbanks, 1970), 7. Lake Pata, Brazil (Colinvaux et al., 1996), 8. Amazon Fan (Maslin et al., 2000; this study), 9. Equatorial Eastern Pacific (Heusser and Shackleton, 1994), 10. Fortaleza, Brazil and North Brazilian Current (Arz et al., 1998, 1999), 11. Huascarán, Peru (Thompson et al., 1995), 12. East Brazil (Auler and Smart, 2001), 13. Sajama, Bolivia (Thompson et al., 1998) and Illumani, Bolivia (Ramirez et al., 2003), 14. Bahia State, Brazil (Wang et al., 2004, 2006, 2007), 15. Lake Titicaca, Peru (Baker et al., 2001a and b; Fritz et al., 2007), 16. South Atlantic Ocean core GeoB 3229-2 (Arz et al., 1998, 1999; Behling et al., 2000, 2002), 17. South Atlantic Ocean core GeoB 3202-1 (Arz et al., 1998, 1999; Behling et al., 2002), 18. Salar de Atacama, Chile (Betancourt et al., 2000; Bobst et al., 2001), 19. Alto Parana, Argentina (Stevaux, 2000), 20. Lakes Lejia and Miscanti, Chile (Grosjean, 1994; Grosjean et al., 2001), 21. Santa Maria Basin and Quebrada del Torro, Argentina (Trauth and Strecker, 1999; Trauth et al., 2000), 22. St8 Santana Cave, Brazil (Cruz et al., 2006, 2009), 23. Colonia, Brazil (Ledru et al., 2005), 24. Botuvera B2, Brazil (Cruz et al., 2006, 2009; Wang et al., 2006), 25. Mar Chiquita, Argentina (Piovano et al., 2008), 26. South East Pacific Ocean core GeoB 3302-1 (Lamy et al., 1999), 27. Salinas Bebedero, Argentina (González, 1994; González and Maidana, 1998), 28. Chilean Lake District, Chile (Heusser, 1989; Markgraf, 1989; Moreno et al., 1999), 29. Cari Laufquen, Argentina (Galloway et al., 1988), 30. Huelmo Site, Chile (Massaferro et al., 2009), 31. Cardiel, Argentina (Stine and Stine, 1990). (For interpretation of the references to colour in this figure legend, the reader is referred to the web version of this article.)

annual precipitation levels in excess of 3600 mm. There is a secondary influence on the strength of the SAMS namely ENSO (Grimm and Ambrizzi, 2009). Changes in the Pacific – Atlantic Ocean temperature gradient can influence the duration and extent of rainfall over Amazonia. El Niño has been linked to prolonged dry season length and thus significant droughts. For example 2005 and 2010 were periods of positive ENSO cycle and Amazon experienced two mega droughts (Lewis et al., 2011). However positive ENSO cycles in 2003 and 2007 did not result in large-scale Amazonian droughts. Equatorial regions play a fundamental role in the transport of heat to the higher latitudes and records of continental palaeoclimate from tropical South America are thus of critical importance in understanding the role played by the Amazon Basin during the Quaternary.

2.1. Site location

The Amazon Fan is a large deep-sea passive margin fan, extending 650–700 km from the continental shelf off the coast of northeastern Brazil. ODP Site 942 (5°45'N, 49°6'W at a water depth of 3346 m) lies adjacent to the main Amazon Fan complex and benefits from the enhanced glacial sedimentation rates which characterise the rest of the Fan complex, whilst also retaining a continuous record with ample pelagic input for climate reconstructions (Flood et al., 1995). The location of Site 942 (Fig. 1) is critical for understanding the meeting and mixing of freshwater discharge from the Amazon River with the local North Brazil Current (NBC) (Maslin et al., 1997; Maslin, 1998; Wilson et al., 2011). The NBC is a warm-water western boundary current which flows northwestwards along the Brazilian continental shelf and acts as a conduit for the cross-equatorial transport of heat and salinity to the North Atlantic Ocean (da Silveira et al., 1994). A seasonal retroflexion of the NBC during boreal summer is related to the seasonal migration of the ITCZ and results in a weakening of northward heat transport across the equator (Johns et al., 1998; Wilson et al., 2011).

Analysis of the diatom fraction of surface sediments from Site 942 reveals that freshwater taxa make up ~75% of the diatom assemblage, compared to just 10%–30% elsewhere on the fan (Mikkelsen et al., 1997). This higher percentage abundance reflects the influence of the freshwater plume discharged by the Amazon River, which is either being transported northward by the NBC, or is breaking away and moving offshore (Maslin et al., 1997; Mikkelsen et al., 1997). Moreover, Wilson et al. (2011) use planktonic foraminiferal oxygen isotopes and Mg/Ca SSTs to show that during the lateglacial period, Younger Dryas, Mid-Holocene and Modern timeslices, ODP Site 942 and surrounding sites consistently exhibit the most negative oxygen isotope values suggesting a continual influence of the Amazon River freshwater plume over this part of the Amazon Fan. The ODP 942 sediments dated to between 22 ka and 10 ka were found to be composed of moderately bioturbated, organic-rich, hemipelagic clays. Magnetic susceptibility records (Flood et al., 1995; Maslin et al., 2000) and visible inspection reveal these core sections to be devoid of turbidites and other signs of reworking that commonly affect such environments. Sediment cores from Site 942 were scanned in detail for any evidence of reworking, including micro-turbidites; the youngest disturbed section found was at about 24 m below sea floor (mbsf), which has been dated at approximately 40 ka (Maslin et al., 2000).

3. Methods

3.1. Age model construction

A new composite age model was developed for ODP Site 942 using a combination of 33 new and published Accelerator Mass

Spectrometry (AMS) radiocarbon (^{14}C) ages (black circles in Fig. 3), that were measured on both multiple- and mono-specific planktonic foraminiferal samples from ODP Holes 942B and 942C as detailed in Table 1. Samples from Hole 942C were measured at the Leibniz-Labor für Alterbestimmung und Isotopenforschung, Kiel University, Germany (Maslin and Burns, 2000; Maslin et al., 2000). Samples from Hole 942B were analysed at the Center for Accelerator Mass Spectrometry, Lawrence Livermore National Laboratory (USA), and also at the Scottish Universities Environmental Research Centre. Each sample measured for ^{14}C was corrected for isotope fractionation through normalization using $\delta^{13}\text{C}$ values measured on the same samples. Measured ^{14}C ages were transferred between Holes using cross-correlated shipboard magnetic susceptibility data (Flood et al., 1995). $\delta^{18}\text{O}$ data from each Hole were also used to refine the synchronisation wherever possible.

In order to translate the ^{14}C chronology into equivalent GISP2 ice core years, non-reservoir corrected ^{14}C ages from ODP Site 942 were correlated with similar data from nearby ODP Site 1002 in the Cariaco Basin (Hughen et al., 2004a) that has been tuned to the GISP2 age scale (Meese et al., 1997). Errors were propagated to incorporate the ^{14}C age errors, GISP2-Cariaco Basin calibration, including the GISP2 count error and the Cariaco Basin-ODP Site 942 calibration. The adoption of a Greenland chronology at ODP Site 942 not only permits direct comparisons to be made with the GISP2

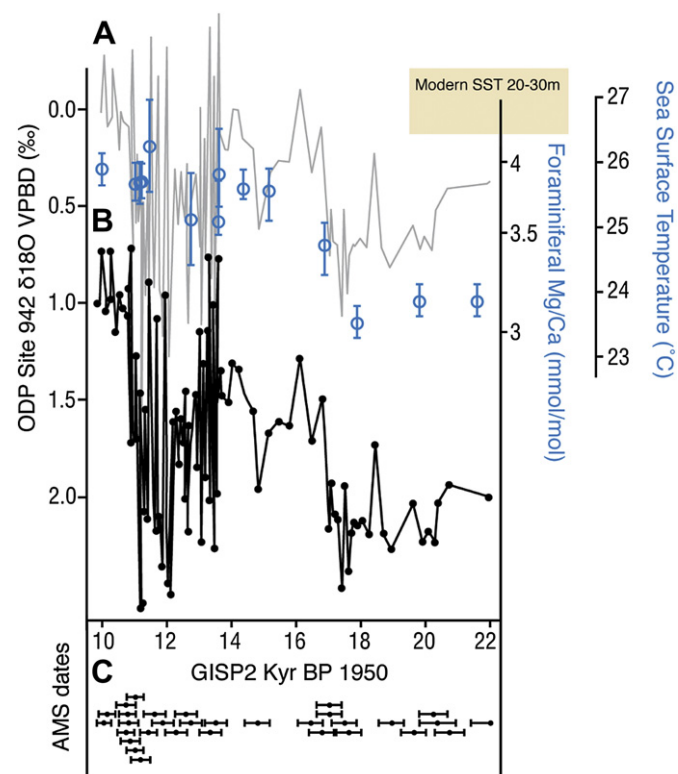


Fig. 2. $\delta^{18}\text{O}$ and sea surface temperature data from ODP Site 942. Blue circles (right axis) represent *G. sacculifer* Mg/Ca ratios and calculated SSTs. Curve A: Light grey line shows the $\delta^{18}\text{O}$ record that has been corrected for the global mean glacioeustatic fractionation (see text and B) using the independently Th/U-dated Barbados sea level record (Peltier and Fairbanks, 2006) scaled to $\delta^{18}\text{O}$, and reflects a composite of changes in both Amazon River outflow history and sea-surface temperature. (B) The Amazon Fan *G. sacculifer* $\delta^{18}\text{O}$ record (dark grey line, left axis) 'raw data' that has been differenced against the 1170 year 'modern' core-top value and offset from curve A by 1‰ to allow better visualisation. (C) Small black diamonds indicate AMS ^{14}C -dated horizons used to tie the ODP Site 942 dataset to the GISP2 age-scale. All data are plotted against GISP2 kyr BP 1950 (Hughen et al., 2004b). (For interpretation of the references to colour in this figure legend, the reader is referred to the web version of this article.)

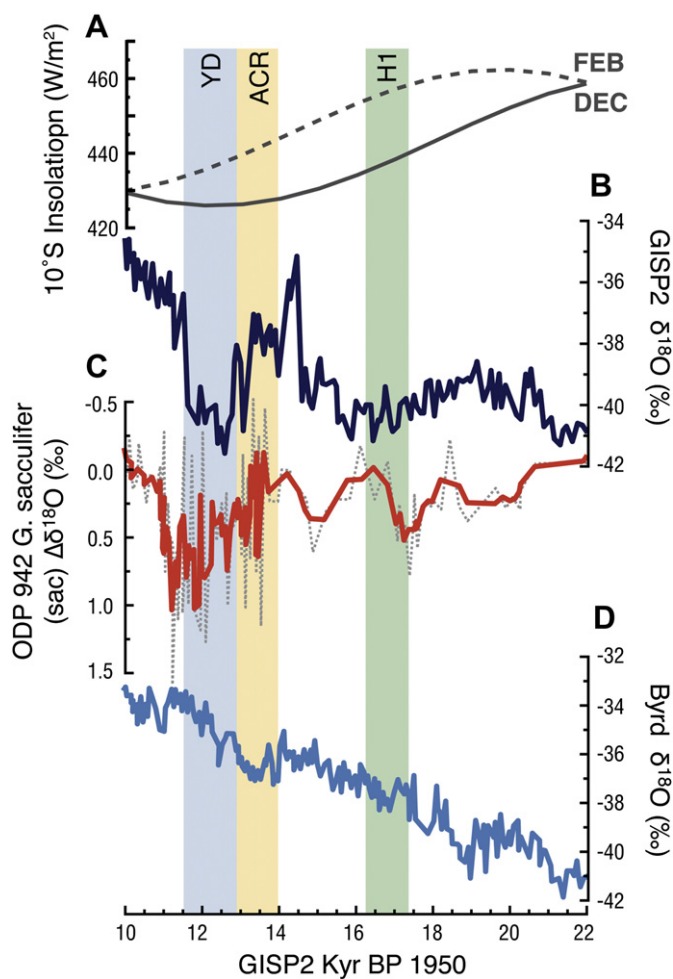


Fig. 3. A comparison between $\Delta\delta^{18}\text{O}$ from ODP Site 942 and $\delta^{18}\text{O}$ from the GISP2 and Byrd ice cores (Blunier and Brook, 2001). (A) solar insolation at 10°S calculated for December and February from Berger and Loutre (1991), coincident with the formation of the Bolivian high atmospheric pressure cell over the Altiplano. (B) GISP2 $\delta^{18}\text{O}$ record from Blunier and Brook (2001) (light blue line). (C) $\Delta\delta^{18}\text{O}$ from on the Amazon Fan that has been corrected for ice volume and temperature fractionation, and differenced against the 1170 year 'modern' core-top value. Red line indicates data that has been smoothed using a three-point moving average, grey line indicates the unsmoothed record with individual data points. More negative values represent a reduction in Amazon river outflow, and hence increased aridity in the Amazon basin. (D) Byrd $\delta^{18}\text{O}$ record that has been methane-synchronised to the GISP2 ice-core shown in (B). ACR = Antarctic cold Reversal and YD = Younger Dryas. (For interpretation of the references to colour in this figure legend, the reader is referred to the web version of this article.)

ice core data, but it also enables correlations to be made with methane-synchronised ice core records from Antarctica (Blunier and Brook, 2001). The Byrd ice core was selected due to its resolved methane-synchronisation record through the deglacial. All ages referred to hereafter are quoted in GISP2 years.

Sedimentation rates calculated from the age model show that between 22.0 and 13.7 ka, sedimentation rates varied between ~ 0.15 and 0.40 m kyr^{-1} , except for between 18.0 and 16.9 ka where there was a period of enhanced accumulation between ~ 0.45 and 3.30 m kyr^{-1} . Sedimentation rates reached a peak of $\sim 5\text{ m kyr}^{-1}$ between 13.8 and 13.5 ka which coincides with an abrupt increase in the abundance of terrestrial detritus in the record. This may be evidence for a shift of the main active channel system towards Site 942 (Maslin et al., 2006) or of a flushing of river sediment following deglaciation in part of the Andes (Maslin and Burns, 2000). Thereafter, until 10.9 ka sediment accumulation rates were approximately

1.35 m kyr^{-1} . At $\sim 10.9\text{ ka}$, sedimentation rates fell abruptly to a more typical oceanic pelagic sedimentation rate of $\sim 0.05\text{ m kyr}^{-1}$, when higher sea levels flooded the continental shelf, and the river deposited its load relatively further inland.

3.2. Planktonic foraminiferal $\delta^{18}\text{O}$ analysis

Cores from ODP Site 942 were sampled every centimetre, giving a sample resolution of between 50 and 5 years depending on changes in the sedimentation rate. This, however, ignores the possible role of bioturbation. If we assume a conservative rate of about 10 cm/ka (Trauth et al., 1997) that suggest the resolution is between 500 and 50 years with an average of 250 years per sample from 22 to 10 ka. Both oxygen and carbon isotopes of planktonic foraminifera were measured. The high sedimentation rates mean that very few if any benthic foraminifera were found. The samples were freeze dried and then wet sieved through a $63\text{ }\mu\text{m}$ mesh sieve, dried in a 60°C oven and weighed. The samples were then dry sieved at convenient intervals between 300 and 355 microns from which 30 individual planktonic foraminiferal tests, which showed no signs of dissolution or reworking, were picked for each species per sample. The five species picked, *Globigerinoides sacculifer* (with sac), *Globigerinoides ruber*, *G. sacculifer* (without sac), *Neogloboquadrina dutertrei*, and *Globorotalia truncatulinoides*, all exhibit a similar pattern and range of isotopic values (Ettwein, 2005).

Samples from 22 to 13.9 ka were measured for $\delta^{18}\text{O}$ and $\delta^{13}\text{C}$ (not shown) using an automated common acid bath VG Isocarb + Optima mass spectrometer at the NERC Isotope Geosciences Laboratory, Keyworth, Nottingham, UK. Samples from 13.9 to 10 ka were measured for $\delta^{18}\text{O}$ using a Finnigan Delta XL + ratio mass spectrometer linked to an Automated Carbonate Prep System (Kiel III) at the Stable Isotope Laboratory, Department of Geosciences, University of Massachusetts, Amherst, USA. All $\delta^{18}\text{O}$ values were measured in per mil (‰), and expressed as deviations relative to the Vienna Pee Dee Belemnite (V-PDB) standard. Analytical sample reproducibility errors were $<0.07\text{‰}$ at each facility, based on replicate measurements of within-run laboratory standards, calibrated against standards from the International Atomic Energy Agency and the National Bureau of Standards. Data from each lab were spliced together and harmonised by comparing the $\delta^{18}\text{O}$ measurements of the laboratory sample standards and inter-laboratory replicate sample data; a correction factor was applied where appropriate.

3.3. Removing the global ice volume effect

The global mean glacioeustatic component of foraminiferal $\delta^{18}\text{O}$ was removed using the independently Th/U-dated Barbados sea level record (EPICA, 2006; Peltier and Fairbanks, 2006) scaled to $\delta^{18}\text{O}$, assuming a modern-LGM amplitude of $\sim 1\text{‰} \pm 0.1\text{‰}$ (Adkins et al., 2002). The Barbados $\delta^{18}\text{O}$ record is considered the best analogue for global ice volume fractionation due to the independent age control of the dataset, coupled with the superior temporal resolution of the record relative to others currently available particularly through the early deglacial interval. In order to remove the glacioeustatic component, $\delta^{18}\text{O}$ from ODP Site 942 were ascribed a calendar year (Cal yr BP) chronology based upon the $15\text{ kyr }^{14}\text{C yr-Cal yr BP}$ calibration from the Cariaco Basin core PL07-58PC (Hughen et al., 2000). Prior to 15 ka, ^{14}C dates were calibrated to calendar years with Calib 5.1 (Stuiver and Reimer, 1993) using the Marine04 marine calibration curve (Hughen et al., 2004b) and incorporating a standard global ocean radiocarbon reservoir correction of ~ 400 years (Stuiver and Reimer, 1993; 2005). The minimum and maximum calendar age ranges for each sample were determined by calculating the probability distribution of the true

Table 1

A table to show the details of the AMS radiocarbon (^{14}C) ages measured for ODP Site 942, with their equivalent ages in GISP2 years BP 1950. Shading represents replicate sample measurement, from which an average of the two ^{14}C ages was taken. Propagated errors incorporate ^{14}C errors, GISP2 count errors, and errors in the Cariaco-GISP2 calibration and Cariaco-Amazon calibration.

AMS Lab and sample code	ODP sample code	942B depth (mbsf)	942C depth (mbsf)	Sample type	^{14}C age (not reservoir corrected)	^{14}C age error +	^{14}C age error -	GISP2 yr BP 1950	Propagated error \pm
KIA 473	942C 1H 1W 80-81		0.80	<i>G. sacculifer</i>	9751	95	95	10199	270
LL CAMS 122186	942B 1H 1W 78-79	0.78		Mixed	9825	35	35	10330	270
KIA 474	942C 1H 1W 88-90		0.88	Mixed	10154	90	90	10903	280
LL CAMS 90540	942B 1H 1W 82-83	0.82		Mixed	10265	35	35	10910	280
LL CAMS 90541	942B 1H 1W 89-90	0.89		Mixed	10205	30	30	10962	280
KIA 5198	942C 1H 1W 97-98		0.98	<i>P. obliquilata</i>	9670	60	60	10977	280
KIA 5197	942C 1H 1W 105-107		1.06	<i>G. trilobus</i> + <i>G. ruber</i> *	10010	60	60	11036	280
KIA 2471	942C 1H 1W 125-129		1.27	Mixed	10800	70	70	11192	290
KIA 2470	942C 1H 1W 125-129		1.27	Mixed	10890	50	50		
KIA 5195	942C 1H 1W 147-150		1.48	Mixed	4690	40	40	11348	290
KIA 2472	942C 1H 2W 30-32		1.81	Mixed	10510	50	50	11592	290
KIA 5193	942C 1H 2W 54-58		2.06	Mixed	10690	60	60	11778	300
KIA 2473	942C 1H 2W 90-92		2.41	Mixed	11650	60	60	12037	300
KIA 5191	942C 1H 2W 143-146		2.94	Mixed	10620	60	60	12430	310
SUERC 8783	942B 1H 3W 33-38	3.35		Mixed	9151	30	30	12741	310
KIA 5189	942C 1H 3W 54-57		3.55	Mixed	11790	70	70	12882	310
LL CAMS 90542	942B 1H 3W 98-100	3.98		Mixed	12180	35	35	13457	320
LL CAMS 89321	942B 1H 4W 38-40	4.89		Mixed	12430	25	25	13642	330
LL CAMS 89322	942B 1H 4W 78-80	5.29		Mixed	12925	30	30	14895	350
SUERC 8784	942B 1H 4W 103-105	5.54		Mixed	13716	45	45	16523	380
LL CAMS 89323	942B 1H 4W 108-110	5.59		Mixed	13875	30	30	16855	380
SUERC 8785	942B 1H 4W 133-135	5.84		Mixed	14419	55	55	17064	390
SUERC 8697	942B 1H 4W 138-140	5.89		Mixed	14478	60	60	17073	390
SUERC 8698	942B 1H 5W 8-10	6.09		Mixed	14733	65	65	17531	390
LL CAMS 89324	942B 1H 5W 23-25	6.24		Mixed	15190	35	35	17674	400
SUERC 8787	942B 1H 5W 38-40	6.39		<i>G. sacculifer</i>	15871	60	60	18,011	650
LL CAMS 89,325	942B 1H 5W 58-60	6.59		Mixed	16,485	35	35	18956	420
SUERC 8788	942B 1H 5W 83-85	6.84		Mixed	17108	70	70	19671	430
LL CAMS 90543	942B 1H 5W 108-110	7.09		Mixed	17840	60	60	20245	460
LL CAMS 90538	942B 1H 5W 113-115	7.14		Mixed	17970	60	60	20365	550
LL CAMS 89326	942B 1H 5W 113-115	7.14		Mixed	18085	50	50		
LL CAMS 90544	942B 1H 5W 120-122	7.21		Mixed	18260	60	60	20724	450
LL CAMS 90539	942B 2H 1W 10-12	7.61		Mixed	17485	50	50	21974	610
LL CAMS 89327	942B 2H 1W 10-12	7.61		Mixed	17535	35	35		

sample age, as this is considered to be a more stable estimate of sample age than the intercept method (Telford et al., 2004). The one-sigma range of the probability distribution was selected as the error term in the radiocarbon ages was fixed at the one-sigma level. Single sample ages were selected by taking the median of the probability distribution.

It should be noted that the ice-volume corrected $\Delta\delta^{18}\text{O}$ record is considered a conservative estimate for a number of reasons. First, the mean ice volume correction does not consider the transient nature of glacial melt-water as it mixes out of Atlantic surface waters (Guilderson et al., 2001). Second, it is difficult to account precisely for deglacial ice volume-related changes in the $\delta^{18}\text{O}$ of surface waters when waning ice sheets are discharging their isotopically-depleted waters into the Atlantic basin (Guilderson et al., 2001). Third and most importantly, glacioeustatic effects will only affect the Atlantic component of the $\Delta\delta^{18}\text{O}$ signal and therefore, by removing ice volume effects from the entire local ambient water $\delta^{18}\text{O}$ signal, there is a potential to overcompensate by an amount equivalent to the volume of freshwater mixed.

3.4. Removing the temperature effect using planktonic foraminiferal Mg/Ca

Between 600 and 900 μg of calcium carbonate was crushed, rinsed and briefly ultrasonicated in ultrahigh quality (UHQ) water nine times, in methanol (Aristar grade) six times, and then again in

UHQ water four times in order to remove clays and fine-grained carbonates. Ferromanganese oxides were also removed with the incorporation of an additional reductive cleaning step and the samples were cleaned again to remove contaminant phases. The samples were screened to determine whether reliable foraminiferal Mg/Ca ratios could be obtained using standard cleaning protocols. Measured Mg/Ca ratios in foraminiferal carbonate can be biased by the presence of clays, detrital grains, adhered carbonates, secondary carbonates and overgrowths, and other contaminant phases. These can be detected using trace element/calcium ratios (including Al/Ca, Fe/Ca, Mn/Ca, Si/Ca, Sr/Ca, and Zn/Ca). Samples were analyzed for trace elements on a Varian Vista inductively-coupled plasma optical emission spectrometer in the Department of Earth Sciences at the University of Cambridge using an intensity ratio calibration. Long-term analytical precision of liquid standards was $\pm 0.4\%$. Replicates of samples that were processed and analysed separately to determine both cleaning reproducibility and sample heterogeneity yielded an average uncertainty of $\pm 2.7\%$ for Mg/Ca (Wilson et al., 2011). Due to low foram abundance, both sac and non-sac forms of *G. sacculifer* were measured for Mg/Ca. Using Mg/Ca is fundamentally advantageous to this study as the Mg/Ca calcification temperature is imprinted simultaneously with the shell $\delta^{18}\text{O}$, so there is no spatial or temporal offset between the two signals (Mashiotto et al., 1999). However there may be a component of temperature fractionation that remains unaccounted for if the foraminiferal Mg/Ca is also responding to changes in sea surface salinity.

4. Results

4.1. Sea surface temperatures

SSTs were calculated using a pre-exponent value of 0.37 and a temperature sensitivity of 0.09 (Dekens et al., 2002). Quoted uncertainties of 1.4 °C incorporate the analytical and Mg/Ca-SST calibration errors and the within-sample variability (Barker et al., 2005). Modern SSTs at ODP Site 942 are 27°–27.5 °C at 20 m water depth, and 26.5° to 27.5 °C at 30 m water depth (Levitus, 1982). Our reconstruction indicates that glacial SSTs were $\sim 23.5^\circ \pm 1.4^\circ \text{C}$, about $3\text{--}4 \pm 1.4^\circ \text{C}$ cooler than modern, and approximately $1.5\text{--}2.5 \pm 1.4^\circ \text{C}$ cooler during the deglacial portion of the record. Between 16 and 10 ka, SSTs were about $1.5\text{--}2.5 \pm 1.4^\circ \text{C}$ cooler than modern and varied by less than 1 °C (Fig. 2). Existing proxy records of glacial western tropical Atlantic SSTs yield conflicting results. Many proxy data support 5° to 6 °C of cooling (Guilderson et al., 1994; Beck et al., 1997), although some records indicate only 0° to 2 °C (Billups and Spero, 1996; Dürkoop et al., 1997) or 2° to 3.5 °C of glacial-interglacial cooling (Bard et al., 1997; Wolff et al., 1998; Wilson et al., 2011).

4.2. Planktonic foraminiferal $\Delta\delta^{18}\text{O}$ record and Amazon River outflow model

Data for *G. sacculifer* (with sac-like final chamber), an abundant mixed layer tropical species (Dekens et al., 2002), yielded the most continuous record of all species analysed and the uncorrected $\delta^{18}\text{O}$ record is displayed in Fig. 2B as the difference from the 1170 year 'modern' core-top value (note this record is also offset by 1‰ from the glacioeustatic corrected record in Fig. 2A so it is easier to see the data). The Glacial to late Holocene uncorrected $\delta^{18}\text{O}$ range is 2.5‰ for *G. sacculifer* and 2.2‰ for *G. ruber* (Ettwein, 2005). This compares with marine records to the east of the Amazon outflow (see point 10 on Fig. 1C), which have a range of 1.9‰ for *G. sacculifer* and 1.6‰ for *G. ruber* (Arz et al., 1999). If we assume that the ice volume and SST effects are broadly similar either side of the Amazon outflow then it suggests the Amazon outflow has an influence of approximately 0.6‰ on the surface water oxygen isotope composition.

In order to isolate the local freshwater impact on surface water salinity, we removed the global mean glacioeustatic component (Fig. 2A) and local Mg/Ca-derived sea surface temperature data (Fig. 2) from the $\delta^{18}\text{O}$ time series as described above. SST changes at ODP Site 942 were scaled to $\delta^{18}\text{O}$ assuming a standard temperature- $\delta^{18}\text{O}$ fractionation of 0.21‰/°C (mean of 0.20–0.22‰ per °C, see Ref. Maslin and Swann, 2005). The isotopic temperature effect was linearly interpolated to the same sample resolution as the foraminiferal $\Delta\delta^{18}\text{O}$ and subtracted from the record. The foraminiferal $\Delta\delta^{18}\text{O}$ record was corrected for temperature fractionation at an equivalent sample resolution through linear interpolation of the SST data. The residual $\Delta\delta^{18}\text{O}$ (red line Fig. 3C) can be explored using a two-component mixing model between an Amazon and a tropical Atlantic Ocean end member, which have average modern-day isotopic values of $\sim -5.5\text{‰}$ and $\sim +1\text{‰}$ respectively (see references in Wilson et al., 2011). Consequently, $\delta^{18}\text{O}$ values at Site 942 will be comprised of a combination of these two isotopic signals dependent on the relative mixing ratio of the two water masses over Site 942. Though these end members will have altered in the past they cannot reverse so the construction of a model of river outflow shows that a relative enrichment (depletion) in the $\Delta\delta^{18}\text{O}$ represents a decrease (increase) in the amount of fresh water mixed over Site 942, arising from changes in the outflow of the Amazon River (Maslin and Burns, 2000). Fig. 2B shows the uncorrected 'raw' foraminiferal $\Delta\delta^{18}\text{O}$ that reveal a strong enrichment during the last glacial period. There is step to more depleted values at about 17 ka

BP. Between 13.6 and 11 ka BP there is a period of more enriched values but also an increase in the variability; this could be in part due to the extremely high resolution through this part of the record. At 11 ka BP there is another step to more depleted values. This general pattern is also reflected in the glacioeustatic correct record shown in Fig. 2A. The pattern though does change when the temperature correction is included (see Fig. 2C) with the colder SST accounting for much of the enrichment in the oxygen isotope record during the last glacial period. Distinct periods of enrichment of this $\Delta\delta^{18}\text{O}$ record occur at 21 to 18 ka BP, 15.5 to 14.5 ka BP and 13.7 to 11 ka BP suggesting that these periods may represent times when the outflow of fresh oxygen isotope depleted Amazon River water was reduced (Maslin and Burns, 2000).

5. Discussion

Fig. 1A shows that rainfall from the modern SASM is drained primarily by the Amazon drainage basin. If we assume, therefore, that the foraminiferal $\Delta\delta^{18}\text{O}$ record at Site 942 is indicative of large-scale changes in Amazon River outflow (Maslin et al., 2000) then the record can be used to infer large-scale changes in moisture availability in at least the eastern and central parts of the Amazon Basin (Maslin and Burns, 2000). Whilst the exact changes in outflow cannot be modelled as the potential changes in the end members remain unknown, there are a number of features that can be noted. The longer-term trends in $\Delta\delta^{18}\text{O}$ broadly follow precession-driven December–February insolation at 10°S (Berger and Loutre, 1991) coincident with the Bolivian High formation and the relative strength of the SASM (Fig. 3).

The $\Delta\delta^{18}\text{O}$ data support a view of increased glacial aridity within the Amazon Basin, although the isotope values show only a slight enrichment relative to today. It has been estimated that the glacial Amazon Basin was up to 5 °C cooler than present (Stute et al., 1995; Colinvaux et al., 1996; Farrera et al., 1999; Vonhof and Kaandorp, 2010) which would have depleted the Amazon River $\delta^{18}\text{O}$ by $\sim 1\text{‰}$ (Dansgaard, 1964), thus biasing the $\Delta\delta^{18}\text{O}$ signal to more negative values. However, a reduction in precipitation may have cancelled out some of this thermodynamic isotopic fractionation via the 'amount effect' (Grootes et al., 1989; Grootes, 1993; Maslin and Burns, 2000; Thompson, 2000; Thompson et al., 2000). The interpretation of a more arid Amazon is supported by 1) inorganic sedimentary lake records from within the Amazon Basin that imply lower water levels or even complete desiccation (e.g., van der Hammen, 1974; Servant et al., 1993; Colinvaux et al., 1996; Ledru et al., 1998; Maslin and Burns, 2000; Sifeddine et al. 2001); 2) oxygen isotope records from speleothems (Breukelen et al., 2008; Cruz et al., 2005, 2009); 3) unweathered plagioclase deposits in the Amazon Fan (Damuth and Fairbanks, 1970; Irion et al., 1995), 4) $\delta^{18}\text{O}$ values of kaolinite within Amazonian soils (Mora and Pratt, 2001) and 5) pollen records from within Amazonia which show that tropical seasonal forest and tropical dry forest occur during the LGM instead of the present tropical rain forest (e.g., Colinvaux, 1989; van der Hammen and Absy, 1994; Marchant et al., 2009) demonstrating a shift to a cold drier climate with temperature reduced by about 4–5 °C and precipitation by about 30% (Farrera et al., 1999). This interpretation is also supported by drier conditions found in northern South America and southern Central America. For example, marine records from the Cariaco Basin clearly show a very dry LGM (Peterson et al., 2000) and Younger Dryas (Haug et al., 2001). Interestingly, the Amazon and Cariaco Basin records become decoupled in the later Holocene as the Amazon gets progressively wetter (Maslin and Burns, 2000; Mayle et al., 2004) while Venezuela becomes progressively drier (Haug et al., 2001).

In contrast other authors have suggested the Amazon Basin was wetter during the last glacial period. Evidence suggested includes

lake level records from the Peruvian/Bolivian Altiplano (Baker et al., 2001a; 2001b), pollen and lake level records from NW Amazonia (Bush et al., 2002) and speleothem evidence from South East Brazil (Wang et al., 2004, 2006; 2007; Cruz et al., 2005, 2006; 2009). However these records are distal and may have been strongly affected by local factors. For example the Peruvian/Bolivian Altiplano (Seltzer, 1990; Seltzer et al., 2000; Baker et al., 2001a; 2001b; Seltzer et al., 2002) records are thought to be driven by increased moisture transport to higher altitudes as the SE winds strengthen (Lenters and Cook, 1997; Marengo and Nobre, 2001; Leduc et al., 2007) following the SASM weakening, while rainfall in the NW Amazonia and SE Brazil are strongly influenced by austral winter rainfall (Cruz et al., 2009). The weight of evidence (see also Refs. Mayle et al., 2009; Sylvestre, 2009), including results from this paper, support the interpretation that the Amazon was more arid during the last glacial period than today (see Fig. 1C for summary).

During the last deglacial period, the $\Delta\delta^{18}\text{O}$ record presented in this paper suggests that maximum aridity occurred during two main time-intervals. One interval, centred at around ~ 20.5 to 17 ka, also features in the records of lowland central America (Hodell et al., 2008) and the Cariaco Basin (Peterson et al., 2000). There is a return to wetter conditions between 17 ka and 16.4 ka, which coincides with Heinrich event H1 (McManus et al., 2004). There is a brief return to more arid conditions around 15 ka. The onset of the second main arid interval (~ 13.6 –11 ka) occurred rapidly between ~ 13.6 and 13.3 ka, coeval with a brief arid period in Central America (Hodell et al., 2008). Fig. 4 shows that this period is coeval with the beginning of the Antarctic Cold Reversal (ACR). The duration of this second dry interval also extends beyond the Northern Hemisphere termination of the Younger Dryas, suggesting that Amazon Basin moisture is not simply a function of Northern high latitude climate. If the Amazon moisture record was simply a response to Northern Hemisphere forcing it would be expected to follow the Cariaco Basin Ti outflow record, which has an arid period that directly corresponds to the Younger Dryas period (Haug et al., 2001).

There is strong variability within the $\Delta\delta^{18}\text{O}$ record from Site 942 during the second arid period, which shows some degree of correlation with the $\delta^{18}\text{O}$ difference between Greenland and Antarctica (i.e. an inter-polar gradient; Fig. 5). This is further corroborated by a simple comparison to rates of change between the tropical and polar gradient datasets, which co-vary on a similar scale. We speculate that the co-variance between the two records is not unrelated, and reflects a tropical-extra tropical climate teleconnection. This is likely associated with the pole-equator temperature gradients within each hemisphere, and their respective influences on the northern and southern boundaries of the SASM convection zone. The control on the position of the ITCZ by the temperature gradient within each Hemisphere is not a new concept and has been demonstrated by modelling work (e.g. Chiang et al., 2003; Chiang and Bitz, 2005; Chiang et al., 2008; Broccoli et al., 2006; Yoshimori and Broccoli, 2008, 2009; Kang et al., 2008, 2009). Two possible explanations are given for this teleconnection. First, when there is a strong temperature gradient (i.e., a large temperature difference over a shorter latitudinal distance) the winds systems become more compressed and the winds are more zonal (east-west). This reduces the ability for winds to be deflected north or south towards the continents and thus reduces moisture transport within monsoonal systems (Broccoli et al., 2006). A second possible reason is that as the Hemispheric temperature gradient cools the extratropics, the atmospheric circulation propagates this cooling into lower latitudes. Heat is required to counter this cooling so the Hadley circulation transports energy into the cooled hemisphere. In the Tropics moisture is carried in the opposite direction as energy, thus the ITCZ shifts

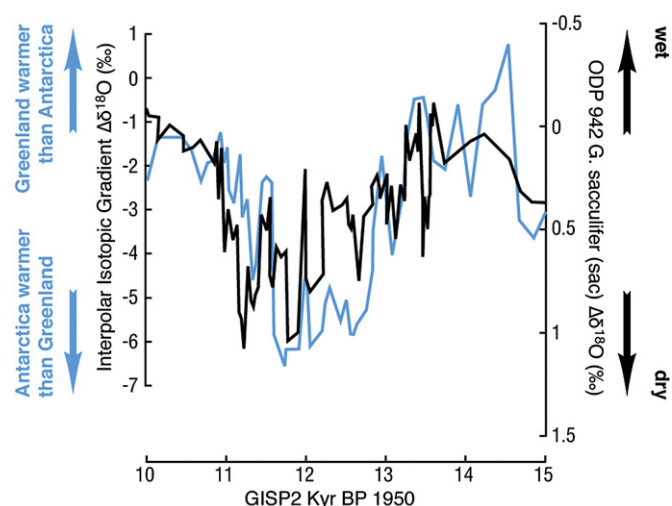


Fig. 4. A comparison between $\Delta\delta^{18}\text{O}$ from ODP Site 942 (black line) and the difference in $\delta^{18}\text{O}$ between GISP2 and Byrd i.e. An inter-polar gradient (blue line). Both datasets have been plotted at the same sample resolution against GISP2 kyr BP 1950 (Hughen et al., 2004b). (For interpretation of the references to colour in this figure legend, the reader is referred to the web version of this article.)

away from the cooled hemisphere (Kang et al., 2008, 2009). This is because moisture is carried only by the lower atmospheric branch of the Hadley cell while the transport of energy is balanced between the upper and lower branches of atmospheric circulation. Kang et al. (2008) also showed that in GCMs the ITCZ position can be highly sensitive to any variation in the climate components that contribute to changes in the atmospheric energy budget, for example, changing cloud properties, melting sea ice, or ocean heat uptake/heat transport changes.

Precipitation within the Amazon Basin originates from the tropical North Atlantic Ocean via the trade winds, which are pulled or deflected into the South American continent by the subtropical high-pressure cells (Barry and Chorley, 1995; Vera et al., 2006). These cells move equator-ward in the cold (winter) hemisphere, and pole-ward in the warm (summer) hemisphere as evidenced today by the directional onset and regression of the summer monsoon season (Vera et al., 2006; Marengo and Nobre, 2001; Lenters and Cook, 1997, see Fig. 1). The popular view of neotropical climate dynamics is that over longer timescales, the continental ITCZ migrates as a static belt in response to Northern Hemisphere temperature change. This view, however, does not fit with the data in this paper or with that of Cruz et al. (2009) who suggested an east to west anti-phasing of climate in South America. Instead we propose that over longer periods, the northern and southern boundaries of the ITCZ migrate *independently* according to the long-term high latitude climatic variations of each respective hemisphere. This produces the east-west anti-phasing observed by Cruz et al. (2009) as their 'Western' South America combines the effect of the movement of the northern and southern SASM boundaries, while their 'Eastern' South America is controlled by just the southern boundary and penetration of the tropical easterlies on to the continent and its associated coastal rainfall. We suggest that moisture availability over the Amazon is a combined effect of long-term precession driven insolation induced changes in SASM intensity (Clement et al., 2004) and the relative independently derived position of the both northern *and* southern boundaries of the ITCZ.

Based on our results from this study and those of other authors, we propose a new testable 'dynamic boundary-monsoon intensity hypothesis' to explain the differences between the glacial, deglacial and modern Amazon Basin moisture levels (Fig. 5). During the LGM,

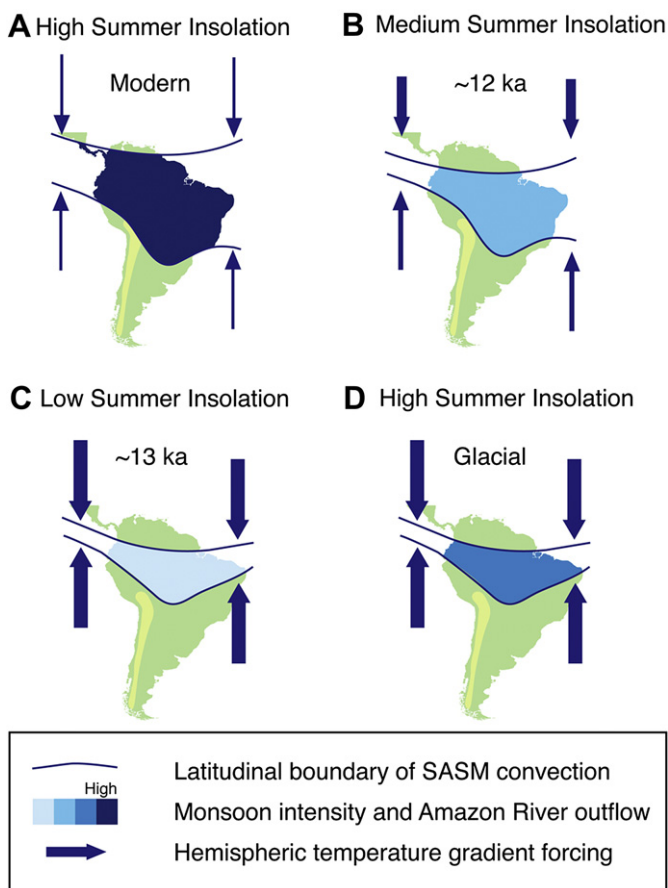


Fig. 5. Cartoon explaining the new dynamic boundary-monsoon intensity hypothesis presented in this study.

we suggest that despite the strong bi-polar temperature gradients and cooler glacial SSTs in the tropical Atlantic, the precessionally-forced near modern insolation levels at 10°S (Clement et al., 2004) would have given rise to a SASM with similar intensity to today. Therefore despite being bi-latitudinally compressed, the glacial SASM would have manifested itself as a zone of intense convective rainfall over the Amazon Basin, with net river outflow enhanced relative to the deglacial period (Fig. 5). During the deglacial period, insolation-driven SASM intensity reduces, but the total area covered by intense rainfall in the Amazon Basin changes due to the movement of either the northern or southern boundaries or both (Fig. 5). We propose this hypothesis both as a way to explain the variability observed within current South American palaeo-data but also as a target that can be tested by future data.

The water balance of South American may provide a pivotal role in generating extratropical feedbacks. Should our dynamic boundary-monsoon intensity hypothesis be correct, it would imply that the southern boundary of the SASM was displaced further southwards across the continental interior at the onset of the ACR. It has been suggested (Peterson et al., 2000; Stansell et al., 2010) that this may have forced the belt of convective rainfall southwards, away from the low-lying Isthmus of Panama and into mountainous Andean terrain. At these latitudes, orographic rainfall and moisture 'blocking' by the Andes could have reduced the freshwater export to the tropical Pacific. Our hypothesis is supported by salinity evidence from the Eastern Equatorial Pacific, which implies a reduction in freshwater export across the Isthmus of Panama during Northern Hemisphere cold intervals (Leduc et al., 2007), including the period coincident with the ACR.

6. Conclusions

The $\Delta\delta^{18}\text{O}$ record from the Site 942 on the western Amazon Fan has a number of important implications. First, it suggests that effective moisture in the Amazon Basin has varied significantly and rapidly between 22 ka and 10 ka. Second, it reinforces the evidence for asynchronous climate change between the hemispheres. Third, it implies that tropical South American climate during the deglacial interval was associated with temperature variations in both the northern and southern high latitudes. Moreover, given the relative phasing of the Antarctic, Amazon and Greenland climate records, it suggests that deglacial climate change in Antarctica and the Amazon Basin preceded a potentially equivalent change in Greenland. Our results also suggest that the effective moisture in the tropics is a combined function of precessional modulated convection and Hemispheric temperature gradients.

Acknowledgements

This work was made possible by the ODP and the efforts of the scientific party and crew of ODP Leg 155. This work formed part of the doctoral dissertation for VJE, under the supervision and funding of MM at University College London. We would like to thank the three reviewers for their detailed and insightful comments, which greatly improved the manuscript. We would like to thank Reviewer 1 for one of the best quotes we have ever received "I think Dr. Maslin is violating some of the fundamental laws of climatology". We thank Juliet Ettwein for assistance with sample material collection, Walter Hale for assistance at the IODP Sample Repository in Bremen, Germany, and members of the ECRC (UCL), NIGL, Department of Earth Sciences Cambridge University (Harry Elderfield and Aradhna Tripathi) and CAMS (LLNL) especially Connie Weyhenmeyer for assistance with sample preparation and measurement. This research was supported by various grants from Natural Environmental Research Council (NERC). Radiocarbon analyses at CAMS were performed under the auspices of the U.S. Department of Energy by the University of California Lawrence Livermore National Laboratory.

References

- Adkins, J.F., McIntyre, K., Schrag, D.P., 2002. The salinity, temperature and $\delta^{18}\text{O}$ of the glacial deep ocean. *Science* 298, 1769–1773.
- Arz, H.W., Patzold, J., Wefer, G., 1998. Correlated millennial-scale changes in surface hydrography and terrigenous sediment yield inferred from last-glacial marine deposits off northeastern Brazil. *Quaternary Research* 50, 157–166.
- Arz, H.W., Patzold, J., Wefer, G., 1999. The deglacial history of the western tropical Atlantic as inferred from high resolution stable isotope records off northeastern Brazil. *Earth and Planetary Science Letters* 167, 105–117.
- Auler, A.S., Smart, P.L., 2001. Late Quaternary paleoclimate in semiarid northeastern Brazil from U-series dating of travertine and water-table speleothems. *Quaternary Research* 55, 159–167.
- Baker, P.A., Rigsby, C.A., Seltzer, G.O., Fritz, S.C., Lowenstein, T.K., Bacher, N.P., 2001a. Tropical climate changes at millennial and orbital timescales on the Bolivian Altiplano. *Nature* 409, 698–701.
- Baker, P.A., Seltzer, G.O., Fritz, S.C., Dunbar, R.B., Grove, M.J., Tapia, P.M., 2001b. The history of South American tropical precipitation for the past 25,000 years. *Science* 291, 640–643.
- Bard, E., Rostek, F., Sonzogni, C., 1997. Interhemispheric synchrony of the last deglaciation inferred from alkenone palaeothermometry. *Nature* 385, 707–710.
- Barker, S., Cacho, I., Benway, H., Tachikawa, K., 2005. Planktonic foraminiferal Mg/Ca as a proxy for past oceanic temperatures: a methodological overview and data compilation for the last glacial maximum. *Quaternary Science Reviews* 24, 821–834.
- Barry, R.G., Chorley, R.J., 1995. *Atmosphere, Weather and Climate*. Routledge, London, p. 397.
- Beck, J.W., Récy, J., Taylor, F., Edwards, R.L., Cabioch, G., 1997. Abrupt changes in early Holocene tropical sea surface temperature derived from coral records. *Nature* 385, 705–707.
- Behling, H., Arz, H.W., Patzold, J., Wefer, G., 2000. Late Quaternary and vegetational dynamics in northeastern Brazil, inferences from marine corals. *Geob 3104-1*. *Quaternary Science Reviews* 19, 981–994.

- Behling, H., Arz, H.W., Pätzold, J., Wefer, G., 2002. Late Quaternary vegetational and climate dynamic in southeastern Brazil, inferences from marine cores GeoB 3229-2 and GeoB 3202-1. *Palaeogeography, Palaeoclimatology, Palaeoecology* 179, 227–243.
- Bendle, J.A., Weijers, J.W.H., Maslin, M.A., Sinninghe Damste, J.S., Schoutan, S., Hopmans, E.C., Boot, C.S., Pancost, R.D., 2010. Major changes in glacial and Holocene terrestrial temperatures and Sources of organic carbon recorded in the Amazon Fan by Tetraethers. *Geochemistry Geophysics Geosystems* 11 Article number Q12007.
- Berger, A., Loutre, M., 1991. Insolation values for the climate of the last 10 million years. *Quaternary Science Reviews* 10, 297–317.
- Betancourt, J.L., Latorre, C., Rech, J.A., Quade, J., Rylander, K.A., 2000. A 22,000-Year record of monsoonal precipitation from Northern Chile's Atacama desert. *Science* 289, 1542–1546.
- Billups, K., Spero, H.J., 1996. Reconstructing the stable isotope geochemistry and paleotemperatures of the equatorial Atlantic during the last 150,000 years: results from individual foraminifera. *Paleoceanography* 11, 217–238.
- Blunier, T., Brook, E.J., 2001. Timing of millennial-scale climate change in Antarctica and Greenland during the last glacial period. *Science* 291, 109–112. doi:10.1126/science.291.5501.109.
- Bobst, A.L., Lowenstein, T.K., Jordan, T.E., et al., 2001. A 106 ka paleoclimate record from drill core of the Salar de Atacama, northern Chile. *Palaeogeography Palaeoclimatology Palaeoecology* 173, 21–42.
- Broccoli, A.J., Dahl, K.A., Stouffer, R.J., 2006. Response of the ITCZ to northern hemisphere cooling. *Geophysical Research Letters* 33, L01702. doi:10.1029/2005GL024546.
- Breukelen, M.R., van Vonhof, H.B., Hellstrom, J.C., Wester, W.C.G., Kroon, D., 2008. Fossil dripwater in stalagmites reveals Holocene temperature and rainfall variation in Amazonia. *Earth and Planetary Science Letters* 275, 54–60.
- Bush, M.B., 2002. On the interpretation of fossil Poaceae pollen in the lowland humid neotropics. *Palaeogeography, Palaeoclimatology, Palaeoecology* 177, 5–17.
- Bush, M.B., Miller, M.C., De Oliveira, P.E., Colinvaux, P.A., 2002. Orbital forcing signal in sediments of two Amazonian lakes. *Journal of Paleolimnology* 27, 341.
- Carvalho, L., Jones, C., Liebmann, B., 2004. The South Atlantic convergence zone: intensity, form, persistence, and relationships with intraseasonal to interannual activity and extreme rainfall. *Journal of Climate* 17, 88–108.
- Chiang, J.C.H., Bitz, C.M., 2005. Influence of high latitude ice cover on the marine intertropical convergence Zone. *Climate Dynamics* 25, 477–496. doi:10.1007/s00382-005-0040-5.
- Chiang, J.C.H., Biasutti, M., Battisti, D.S., 2003. Sensitivity of the Atlantic ITCZ to last glacial maximum boundary conditions. *Paleoceanography* 18. doi:10.1029/2003PA000916.
- Chiang, J.C.H., Cheng, W., Bitz, C.M., 2008. Fast teleconnections to the tropical Atlantic sector from Atlantic thermohaline adjustment. *Geophysical Research Letters* 35, L07704. doi:10.1029/2008GL03292.
- Clement, A.C., Hall, A., Broccoli, A.J., 2004. The importance of precessional signals in the tropical climate. *Climate Dynamics* 22, 327–341.
- Colinvaux, P.A., 1989. Ice-age Amazon revisited. *Nature* 340, 188–189.
- Colinvaux, P.A., De Oliveira, P.E., Moreno, J.E., Miller, M.C., Bush, M.B., 1996. A long pollen record from lowland Amazonia: forest and cooling in glacial times. *Science* 274, 85–88.
- Cook, K., 2009. South American climate variability and change: remote and regional forcing processes in past climate variability in South America and surrounding regions: from the last glacial maximum to the Holocene. In: Vimeux, F., Sylvestre, F., Khodri, M. (Eds.), *Developments in Paleoenvironmental Research*. Springer, Dordrecht, The Netherlands, pp. 193–212.
- Cruz, F.W., et al., 2005. Insolation-driven changes in atmospheric circulation over the past 116,000 years in subtropical Brazil. *Nature* 434, 63–66.
- Cruz, F.W., Burns, S.J., Karmann, I., Sharp, W.D., Vuille, M., 2006. Reconstruction of regional atmospheric circulation features during the late Pleistocene in subtropical Brazil from oxygen isotope composition of speleothems. *Earth and Planetary Science Letters* 248, 495–507.
- Cruz, F.W., Vuille, M., Burns, S.J., Wang, X., Cheng, H., Werner, M., Edwards, R.L., Karmann, I., Auler, A.S., Nguyen, H., 2009. Orbital driven east-west antiphasing of South American precipitation. *Nature Geoscience* 2, 210–214.
- da Silveira, I.C.A., de Miranda, L.B., Brown, W.S., 1994. On the origins of the north Brazil current. *Journal of Geophysical Research* 99, 22501–22512.
- Damuth, J.E.D., Fairbanks, R., 1970. Late Quaternary sedimentation in the western equatorial Atlantic Source. *Geological Society of America Bulletin* [0016-7606] 88, 695–710.
- Dansgaard, W., 1964. Stable isotopes of precipitation. *Tellus* 16, 436–469.
- Dekens, P.S., Lea, D.W., Pak, D.K., Spero, H.J., 2002. Core top calibration of Mg/Ca in tropical foraminifera: refining paleotemperature estimation. *Geochemistry, Geophysics, Geosystems* 3. doi:10.1029/2001GC000200.
- Dürkoop, A., Hale, W., Mulitza, S., Pätzold, J., Wefer, G., 1997. Late Quaternary variations of sea surface salinity and temperature in the western tropical Atlantic: evidence from $\delta^{18}\text{O}$ of *Globigerinoides sacculifer*. *Paleoceanography* 12, 764–772.
- EPICA Community Members, 2006. One-to-one coupling of glacial climate variability in Greenland and Antarctica. *Nature* 444, 195–198. doi:10.1038/nature/05301.
- Ettwein, V., 2005. The Effective Moisture History of the Amazon Basin for the Last 40,000 years Reconstructed from ODP Site 942 on the Amazon Fan. PhD University College, London, p. 241.
- Farrera, I., et al., 1999. Tropical climates at the last glacial maximum: a new synthesis of terrestrial paleoclimate data. I. vegetation, lake-levels and geochemistry. *Climate Dynamics* 15, 823–856.
- Flood, R.D., et al., 1995. Proceedings of the ODP Program, Initial Reports 155 College Station, TX (ODP).
- Franzinelli, E., Potter, P.E., 1983. Petrology, chemistry, and texture of modern river sands, Amazon River system. *The Journal of Geology* 91, 23–39.
- Fritz, S.C., Baker, P.A., Seltzer, G.O., et al., 2007. Quaternary glaciation and hydrologic variation in the South American tropics as reconstructed from the Lake Titicaca drilling project. *Quaternary Research* 68, 410–420.
- Galloway, R.W., Markgraf, V., Bradbury, J.P., 1988. Dating shorelines of lakes in Patagonia, Argentina. *Journal of South American Earth Sciences* 1, 195–198.
- González, M.A., 1994. Salinas del Bebedero Basin (República Argentina). In: Kelts, K., Gierlowski-Cordes, E. (Eds.), *Global Inventory of Lake Basins*. Cambridge University Press.
- González, M.A., Maidana, N., 1998. Post-Wisconsinian paleoenvironments at Salinas del Bebedero basin, San Luis, Argentina. *Journal of Paleolimnology* 20, 353–368.
- Grimm, A.M., Ambrizzi, T., 2009. Chapter 7 teleconnections into South America from the tropics and extratropics on interannual and intraseasonal timescales, in past climate variability in South America and surrounding regions: from the last glacial maximum to the Holocene. In: Vimeux, F., Sylvestre, F., Khodri, M. (Eds.), *Developments in Paleoenvironmental Research*. Springer, Dordrecht, The Netherlands, pp. 159–192.
- Groote, P.M., 1993. In: Swart, P.K., Lohmann, K.C., McKenzie, J., Savin, S. (Eds.), *Climate Change in Continental Isotopic Records*, vol. 78. AGU, Washington, pp. 37–46.
- Groote, P.M., Stuiver, M., Thompson, L.G., Mosley-Thompson, E., 1989. Oxygen isotope changes in tropical ice, Quelccaya, Peru. *Journal of Geophysical Research* 94, 1187–1194.
- Grosjean, M., 1994. Paleohydrology of the laguna Lejía (north Chilean Altiplano) and climatic implications for lateglacial times. *Palaeogeography Palaeoclimatology Palaeoecology* 109, 89–100.
- Grosjean, M., van Leeuwen, J.F.N., van der Knaap, W.O., et al., 2001. A 22,000 14C year BP sediment and pollen record of climate change from Laguna Miscanti (23°S), northern Chile. *Global and Planetary Change* 28, 35–51.
- Guilderson, T.P., Fairbanks, R.G., Rubenstone, J.L., 1994. Tropical temperature variations since 20,000 years ago: modulating interhemispheric climate change. *Science* 263, 663–665.
- Guilderson, T.P., Fairbanks, R.G., Rubenstone, J.L., 2001. Tropical Atlantic coral oxygen isotopes: glacial-interglacial sea surface temperatures and climate change. *Marine Geology* 172, 75–89.
- Haberle, S., Maslin, M.A., 1999. Late Quaternary Vegetation and climate changes in the Amazon basin based on a 50,000 year pollen record from the Amazon Fan ODP Site 931. *Quaternary Research* 51, 27–38.
- Haug, G.H., Hughen, K.A., Sigman, D.M., Peterson, L.C., Röhl, U., 2001. Southward migration of the intertropical convergence zone through the Holocene. *Science* 293, 1304–1308.
- Heusser, C.J., 1989. Southern Westerlies during the last glacial maximum. *Quaternary Research* 31, 423–425.
- Heusser, L.E., Shackleton, N.J., 1994. Tropical climatic variation on the Pacific slopes of the Ecuadorian Andes based on a 25,000-year pollen record from deep-sea sediment core Tri 163–31B. *Quaternary Research* 42, 222–225.
- Hodell, D.A., et al., 2008. An 85-ka record of climate change in lowland Central America. *Quaternary Science Reviews* 27, 1152–1165.
- Hughen, K.A., Overpeck, J.T., Peterson, L.C., Trumbore, S., 1996. Rapid climate changes in the tropical Atlantic region during the last deglaciation. *Nature* 380, 51–54.
- Hughen, K.A., Southon, J.R., Lehman, S.J., Overpeck, J.T., 2000. Synchronous radiocarbon and climate shifts during the last deglaciation. *Science* 290, 1951–1954.
- Hughen, K.A., et al., 2004a. ^{14}C activity and global carbon cycle changes over the past 50,000 years. *Science* 303, 202–207.
- Hughen, K.A., et al., 2004b. Marine04 Marine radiocarbon age calibration 26–0 ka BP. *Radiocarbon* 46, 1059–1086.
- Irion, G., Müller, J., Nunes de Mello, J., Junk, W.J., 1995. Quaternary geology of the Amazonian lowlands. *Geo-Marine Letters* 15, 172–178.
- Islebe, G.A., Hooghiemstra, H., van der Borg, K., 1995. A cooling event during the Younger Dryas Chron in Costa Rica. *Palaeogeography, Palaeoclimatology, Palaeoecology* 117, 73–80.
- Johns, W.E., Lee, T.N., Beardsley, R.C., Candela, J., Limeburner, R., Castro, B., 1998. Annual cycle and variability of the north Brazil current. *Journal of Physical Oceanography* 28, 103–128.
- Kang, S.M., Held, I.M., Frierson, D.M.W., Zhao, M., 2008. The response of the ITCZ to extratropical thermal forcing: idealized slab-ocean experiments with a GCM. *Journal of Climate* 21, 3521–3532.
- Kang, S.M., Frierson, D.M.W., Held, I.M., 2009. The tropical response to extratropical thermal forcing in an idealized GCM: the importance of radiative feedbacks and convective parameterization. *Journal of the Atmospheric Sciences* 66, 2812–2827. doi:10.1175/2009JAS2924.1.
- Kodama, Y.M., 1992. Large-scale common features of subtropical precipitation zones (the Baiu frontal zone, the SPZ, and the SACZ). part I: characteristics of subtropical frontal zones. *Journal of The Meteorological Society of Japan* 70, 813–835.
- Lamy, F., Hebbeln, D., Wefer, G., 1999. High-resolution marine record of climatic change in midlatitude Chile during the last 28,000 years based on terrigenous sediment parameters. *Quaternary Research* 51, 83–93.

- Lea, D.W., Pak, D.K., Peterson, L.C., Hughen, K.A., 2003. Synchronicity of tropical and high-latitude Atlantic temperatures over the last glacial termination. *Science* 301, 1361–1364.
- Ledru, M.P., Bertaux, J., Sifeddine, A., 1998. Absence of last glacial Maximum records in lowland tropical forests. *Quaternary Research* 49, 233–237.
- Ledru, M.P., Rousseau, D.D., Cruz, J.F.W., et al., 2005. Paleoclimate changes during the last 100 ka from a record in the Brazilian Atlantic rainforest region and interhemispheric comparison. *Quaternary Research* 64, 444–450.
- Leduc, G., et al., 2007. Moisture transport across Central America as a positive feedback on abrupt climate changes. *Nature* 445. doi:10.1038/nature05578.
- Lenters, J.D., Cook, K.H., 1997. On the origin of the Bolivian high and related circulation features of the South American climate. *Journal of the Atmospheric Sciences* 54, 656–677.
- Levitus, S., 1982. Ocean Maps. National Ocean and Atmosphere Administration (NOAA).
- Lewis, S., et al., 2011. The 2010 Amazon Drought. *Science* 331, 554.
- Leyden, B., 1985. Late Quaternary aridity and Holocene moisture fluctuations in the Lake Valencia Basin, Venezuela. *Ecology* 66, 1279–1295.
- Marchant, R., et al., 2009. Pollen-based biome reconstructions for Latin America at 0, 6000 and 18 000 radiocarbon years ago. *Climate of The Past* 5, 725–767. www.clim-past.net/5/725/2009/.
- Marengo, J.A., Nobre, C.A., 2001. General characteristics and variability of climate in the Amazon Basin. In: McClain, M.E., Victoria, R.L., Richey, J.E. (Eds.), *The Biogeochemistry of the Amazon Basin*. Oxford University Press, Oxford, pp. 17–41.
- Markgraf, V., 1989. Reply to Heusser's 'Southern Westerlies during the last glacial maximum'. *Quaternary Research* 31, 426–432.
- Mashiotta, T.A., Lea, D.W., Spero, H.J., 1999. Glacial-interglacial changes in subantarctic sea surface temperature and $\delta^{18}\text{O}$ -water using foraminiferal Mg. *Earth and Planetary Science Letters* 170, 417–432.
- Maslin, M.A., 1998. Equatorial Western Atlantic Ocean circulation changes linked to the Heinrich events: deep-sea sediment evidence from the Amazon Fan. In: Cramp, A., MacLeod, C.J., Lee, S., Jones, E.J.W. (Eds.), *Geological Evolution of Ocean Basins: Results from the Ocean Drilling Program*. Geological Society, London, Special Publications, vol. 131, pp. 111–127.
- Maslin, M.A., Burns, S.J., 2000. Reconstruction of the Amazon Basin effective moisture availability over the past 14,000 years. *Science* 290, 2285–2287.
- Maslin, M.A., Swann, G., 2005. Isotopes in marine sediments. In: Leng, M. (Ed.), *Isotopes in Palaeoenvironmental Research*. Springer, Dordrecht, The Netherlands, pp. 227–290.
- Maslin, M.A., Burns, S., Erlenkeuser, H., Hohnemann, C., 1997. Stable Isotope Records from ODP Sites 932 and 933, ODP Leg 155 Scientific Results Volume, pp. 305–318.
- Maslin, M.A., et al., 2000. Palaeoreconstruction of the Amazon River freshwater and sediment discharge using sediments recovered at site 942 on the Amazon Fan. *Journal of Quaternary Science* 15, 419–434.
- Maslin, M.A., Mahli, Y., Phillips, O., Cowling, S., 2005. New views on an old forest: assessing the longevity, resilience and future of the Amazon Rainforest. *Transactions of the Institute of British Geographers* 30, 390–401.
- Maslin, M.A., Knutz, P.C., Ramsay, T., 2006. Millennial-scale sea level control on Avulsion events on the Amazon Fan, critical Quaternary Stratigraphy Special Issue. *Quaternary Science Review* 25, 3338–3345.
- Massaferro, J.I., Moreno, P.I., Denton, G.H., et al., 2009. Chironomid and pollen evidence for climate fluctuations during the last glacial termination in NW Patagonia. *Quaternary Science Review* 28, 517–525.
- Mayle, F.E., Beerling, D.J., Gosling, W.D., et al., 2004. Responses of Amazonian ecosystems to climatic and atmospheric CO₂ changes since the last glacial maximum. *Philosophical Transactions of The Royal Society B* 359, 499–514.
- Mayle, F.E., Burn, M.J., Power, M., et al., 2009. Vegetation and fire at the last glacial maximum in tropical South America. In past climate variability in South America and surrounding regions: from the last glacial maximum to the Holocene. In: Vimeux, F., Sylvestre, F., Khodri, M. (Eds.), *Developments in Paleoenvironmental Research*. Springer, Dordrecht, The Netherlands, pp. 89–112.
- McManus, J.F., Francois, J.M., Gherardi, L.D., Keigwin, L.D., Brown-Leger, S., 2004. Collapse and rapid resumption of Atlantic meridional circulation linked to deglacial climate changes. *Nature* 428, 834–837. doi:10.1038/nature02494.
- Meese, D.A., et al., 1997. The Greenland ice Sheet project 2 depth-age scale: methods and results. *Journal of Geophysical Research* 102, 26411–26423.
- Mikkelsen, N., Maslin, M.A., Giraudeau, J., Showers, W., 1997. Biostratigraphy and sedimentation rates of the Amazon Fan. In: Flood, R.D., Piper, D.J.W., Klaus, A., Peterson, L.C. (Eds.), *Proceedings of the Ocean Drilling Program, Scientific Results*, vol. 155. Ocean Drilling Program, College Station, TX, pp. 577–594.
- Milliman, J.D., Meade, R.H., 1983. World-wide delivery of river sediments to the oceans. *Journal of Geology* 91, 1–21.
- Mora, C., Pratt, L.M., 2001. Isotopic evidence for cooler and drier conditions in the tropical Andes during the last glacial stage. *Geology* 29, 519–522.
- Moreno, P.I., Lowell, T.V., Jacobson, G.L., Denton, G.H., 1999. Abrupt vegetation and climate changes during the last glacial maximum and last termination in the Chilean Lake District: a case study from Canal de la Puntilla (41°S). *Geografiska Annaler* 81, 285–311.
- Peltier, W.R., Fairbanks, R.G., 2006. Global glacial ice volume and last glacial maximum duration from an extended Barbados sea level record. *Quaternary Science Reviews*. doi:10.1016/j.quatsciv.2006.04.010.
- Peterson, L.C., Haug, G.H., Hughen, K.A., Ruhl, U., 2000. Rapid changes in the hydrologic cycle of the tropical Atlantic during the last glacial. *Science* 290, 1947–1951.
- Piovano, E., Ariztegui, D., Córdoba, F., et al., 2008. Reconstrucciones paleohidrologicas en la región pampeana (Programa paleo-pampas) XII Argentine Meeting of Sedimentology, XIIRAS, Buenos Aires, Argentina.
- Ramirez, E., Hoffman, G., Taupin, J.D., et al., 2003. A new Andean deep ice core from Nevado Illimani (6350 m), Bolivia. *Earth and Planetary Science Letters* 212, 337–350.
- Seltzer, G.O., 1990. Recent glacial history and palaeoclimate of the Peruvian-Bolivian Andes. *Quaternary Science Review* 9, 137–152.
- Seltzer, G.O., Rodbell, D.T., Burns, S.J., 2000. Isotopic evidence for late Quaternary climatic change in tropical South America. *Geology* 28, 35–38.
- Seltzer, G.O., Rodbell, D.T., Baker, P.A., Fritz, S.C., Tapia, P.M., Rowe, H.D., Dunbar, R.B., 2002. Early warming of tropical South America at the last glacial-interglacial transition. *Science* 296, 1685–1686.
- Servant, M., Maley, J., Turcq, B., Absy, M., Brenac, P., Fournier, M., Ledru, M.-P., 1993. Tropical forest changes during the late Quaternary in African and South American lowlands. *Global and Planetary Change* 7, 25–40.
- Sifeddine, A., Martin, L., Turcq, B., Volkermer-Ribero, C., Soubies, F., Cordeiro, R.C., Suguio, K., 2001. Variations in the Amazonian rain forest environment: a sedimentological record covering 30,000 years. *Palaeogeography, Palaeoclimatology, Palaeoecology* 168, 221–235.
- Stansell, N., et al., 2010. Abrupt Younger Dryas cooling in the northern tropics recorded in lake sediments from the Venezuelan Andes. *Earth and Planetary Science Letters* 293, 154–163.
- Stevaux, J.C., 2000. Climatic events during the late Pleistocene and Holocene in the Upper Parana River: correlation with the NE Argentina and South-Central Brazil. *Quaternary International* 72, 73–85.
- Stine, S., Stine, M., 1990. A record from Lake Cardiel of climate change in southern South America. *Nature* 345, 705–707.
- Stuiver, M., Reimer, P.J., 1993. Extended ¹⁴C database and revised CALIB radiocarbon calibration program (Version 5.0). *Radiocarbon* 35, 215–230.
- Stuiver, M., Reimer, P.J., Reimer, R., 2005. CALIB Manual. <http://radiocarbon.pa.qub.ac.uk/calib/manual/>.
- Stute, M., et al., 1995. Cooling of tropical Brazil (5°C) during the last glacial maximum. *Science* 269, 379–383.
- Sylvestre, F., 2009. Moisture pattern during the last glacial maximum in South America. In past climate variability in South America and surrounding regions: from the last glacial maximum to the Holocene. In: Vimeux, F., Sylvestre, F., Khodri, M. (Eds.), *Developments in Paleoenvironmental Research*. Springer, Dordrecht, The Netherlands, pp. 3–27.
- Telford, R.J., Heegaard, E., Birks, H.J.B., 2004. The intercept is a poor estimate of a calibrated radiocarbon age. *The Holocene* 14, 296–298.
- Thompson, L.G., 2000. Ice core evidence for climate change in the Tropics: implications for our future. *Quaternary Science Reviews* 19, 19–34.
- Thompson, L.G., Mosley-Thompson, E., Davis, M.E., et al., 1995. Lateglacial stage and Holocene tropical ice core records from Huascarán, Peru. *Science* 269, 46–50.
- Thompson, L.G., Davis, M.E., Mosley-Thompson, E., et al., 1998. A 25,000-year tropical climate history from Bolivian ice cores. *Science* 282, 1858–1864.
- Thompson, L.G., Mosley-Thompson, E., Henderson, K.A., 2000. Ice-core palaeoclimate records in tropical South America since the last glacial maximum. *Journal of Quaternary Science* 15, 377–394.
- Trauth, M.H., Strecker, M.R., 1999. Formation of landslide-dammed lakes during a wet period between 40,000 and 25,000 yr B.P. in northwestern Argentina. *Palaeogeography, Palaeoclimatology, Palaeoecology* 153, 277–287.
- Trauth, M.H., Sarnthein, M., Arnold, M., 1997. Bioturbational mixing depth and carbon flux at the seafloor. *Paleoceanography* 12, 517–526.
- Trauth, M.H., Ricardo, A.A., Haselton, K.R., et al., 2000. Climate change and mass movements in the NW Argentine Andes. *Earth and Planetary Science Letters* 179, 243–256.
- van der Hammen, T., 1974. The Pleistocene changes of vegetation and climate in tropical South America. *Journal of Biogeography* 1, 3–26.
- van der Hammen, T., Absy, M.L., 1994. Amazonia during the last glacial. *Palaeogeography, Palaeoclimatology, Palaeoecology* 109, 247–261.
- van der Hammen, T., Hooghiemstra, H., 2003. Interglacial-glacial Fuquene-3 pollen record from Colombia: an Eemian to Holocene climate record. *Global and Planetary Change* 36, 181–199.
- Vera, C.W., et al., 2006. Towards a unified view of the American monsoon systems. *Journal of Climate* 19, 4977–5000.
- Vonhof, H.B., Kaandorp, R.J.G., 2010. Climate variations in Amazonia during the Neogene and the Quaternary. In: Hoorn, C., Wesselingh, F. (Eds.), *Amazonia: Landscape and Species Evolution*. Wiley-Blackwell, pp. 201–210.
- Wang, X., et al., 2004. Wet periods in northeastern Brazil over the past 210 kyr linked to distant climate anomalies. *Nature* 432, 740–743.
- Wang, X., et al., 2006. Interhemispheric anti-phasing of rainfall during the last glacial period. *Quaternary Science Review* 25, 3391–3403.
- Wang, X., et al., 2007. Millennial-scale precipitation changes in southern Brazil over the past 90,000 years. *Geophysical Research Letters* 241, 699–706.
- Wilson, K.E., Maslin, M.A., Burns, S.J., 2011. Evidence for a prolonged retroflexion of the North Brazil Current during glacial stages. *Palaeogeography, Palaeoclimatology, Palaeoecology*. doi:10.1016/j.palaeo.2011.01.003.

- Wolff, T., Mulitza, S., Arz, H.W., Wefer, G., 1998. Oxygen isotopes versus CLIMAP (18 ka) temperatures: a comparison from the tropical Atlantic. *Geology* 26, 675–678.
- Yoshimori, M., Broccoli, A.J., 2008. Equilibrium response of an atmosphere-mixed layer ocean model to different radiative forcing agents: global and zonal mean response. *Journal of Climate* 21, 4399–4423. doi:10.1175/2008JCLI2172.1.
- Yoshimori, M., Broccoli, A.J., 2009. On the link between Hadley circulation changes and radiative feedback processes. *Geophysical Research Letters* 36 (L20), 703. doi:10.1029/2009GL040488.
- Zhou, J., Lau, K.-M., 1998. Does a monsoon climate exist over South America? *Journal of Climate* 11, 1020–1040.